



## Biodegradation of Azo Dyes in Synthetic Medium and Textile Effluent using a Potent Bacterium *Bacillus* sp. TDS50 and its Extracellular Metabolites

DIVYA MUTHARASU<sup>1</sup>, RAJAKUMAR SUNDARAM<sup>2,1b</sup> and AYYASAMY PUDUKKADU MUNUSAMY<sup>1,\*</sup>

<sup>1</sup>Department of Microbiology, Periyar University, Salem-636011, India

<sup>2</sup>Department of Marine Biotechnology, Bharathidasan University, Tiruchirappalli-620024, India

\*Corresponding author: E-mail: [pmayyasamy@gmail.com](mailto:pmayyasamy@gmail.com)

Received: 21 May 2025;

Accepted: 16 July 2025;

Published online: 31 July 2025;

AJC-22080

Azo dyes in textile effluents, pose substantial environmental problems owing to their persistence, toxicity and potential to form harmful carcinogenic and mutagenic byproducts, like aromatic amines. This study aimed to evaluate the degradation of reactive red (RR) and reactive blue (RB) azo dyes by an indigenous bacterial strain (*Bacillus* sp. TDS50) isolated from textile industry effluent. The *Bacillus* sp. TDS50, showed the highest decolorization efficiency of 98.30% for RR and 98.02% for RB. The strain showed its significant decolorization of azo dyes using glucose as a carbon source, pH 7, temperature 35 °C, dye concentration 100 mg/L and an inoculum size 1%. A laboratory scale bioreactor was used to decolourize the dyes under optimum conditions. An analytical study of the degraded product was performed using FTIR spectroscopy and gas chromatography-mass spectroscopy (GC-MS). Another major focus of this investigation was decolourization in an aqueous medium using bacterially produced extracellular metabolites, viz. biofloculants (BF) and biosurfactants (BS). The results of the bacterial treatment followed by phytotoxicity indicated the non-toxic nature of the treated effluent compared to untreated effluents.

**Keywords:** *Bacillus* sp. TDS50, Decolourization, Azo dyes, Bioreactor, Biofloculants, Biosurfactants.

### INTRODUCTION

Numerous industries, including food, cosmetics, paper printing and pharmaceuticals, heavily rely on the synthetic azo dyes. However, the largest consumer of these products is chemical industries [1]. The organic load and toxicity of textile wastewater are increased by dyes, which are often aromatic heterocyclic compounds that are frequently resistant to organic molecules that cause colour change. Aromatic primary amines are often diazotized and subsequently joined with one or more nucleophiles, which are electron-rich molecules, such as amino acids and hydroxy acids [2]. About 50% of commercial dyes used in the industries are azo dyes [3].

Azo dyes in plant cause toxicity, mutagenicity and carcinogenicity. They also hinder plant growth, enter the food chain, produce recalcitrance and cause bioaccumulation [4]. The dyes in water have an apparent colour, which alters their transparency and esthetics, preventing light from penetrating and lowering the concentration of dissolved oxygen [4-6]. Synthetic

dyes can inhibit the growth of bacteria, protozoa, plants, animals and humans. They can also cause allergies, tumors and malignancies [7]. Dye containing wastewater can be effectively treated using a variety of methods, including chemical treatment, absorption, filtration, biological treatment and coagulation [4,8]. Thus, given their cost-effectiveness and environmental friendliness, biological treatment techniques utilizing microorganisms appear to be the best substitutes for physico-chemical techniques [5,6].

Biological approaches have gained increased attention as viable treatments for dyeing wastewater because of their high efficiency, low cost and environmental friendliness [9]. Microorganisms have long been known to decolourize and metabolize azo dyes, which has increased interest in the use of bioremediation based systems for treating textile wastewater [6]. In bioremediation, decolourized azo dyes are absorbed by microorganisms such as bacteria, algae, yeast and filamentous fungi [10]. Bioremediation has drawn increased attention because it is a more promising approach than physical and chemical ther-

apies and the byproducts of bacterial metabolites are often non-toxic [4].

Microorganisms in the growth phase produce biopolymers known as bioflocculant (BF). Bioflocculants are easily degradable and are less hazardous to the environment [11]. They are made up of intricate multi-chain molecular polymers that include proteins, glycoproteins, sugar derivatives and repeated branching polyols [12]. Similarly, biosurfactants (BS) are amphiphilic biological compounds produced from various filamentous fungi, bacteria and yeasts, either extracellularly or as part of their cell membranes [13,14]. These molecules have amphiphilic properties due to the structure they have, which consists of a hydrophilic head (peptides, amino acids and polysaccharides) and a hydrophobic tail (saturated and unsaturated fatty acids) [15]. Biosurfactants is characterized by enhanced biodegradability, enhanced environmental biocompatibility, enhanced performance under extreme temperature, pH and salinity conditions and non-toxicity [15,16]. Biosurfactants reduces surface tension, critical micelle concentration (CMC) and interfacial tension in hydrocarbon mixtures and aqueous solutions [17]. The present study focused on the biological removal of azo dyes from contaminated water using live bacteria and their extracellular metabolites (BF and BS). In this work, an indigenous bacterial strain (*Bacillus* sp. TDS50) isolated from textile industry wastewater was tested for its degradation of reactive red (RR) and reactive blue (RB) azo dyes under the optimized conditions.

## EXPERIMENTAL

The azo dyes reactive red (RR) and reactive blue (RB) were obtained from a textile industry in Erode, India. All chemicals used in this study were purchased from different sources like HiMedia Laboratories Pvt Ltd., Sisco Research Laboratories Pvt. Ltd. and Thermo Fisher Scientific Company, India.

**Isolation and screening of RR and RB dye-degrading bacteria:** Azo dye-degrading bacteria were isolated from the textile effluent and soil samples near the industrial plant located in the Erode and Tiruppur districts, India. To isolate the potential azo dye-degrading bacterial strains from the soil and sediment samples, the spread plate technique was employed using LB agar plates and incubated at  $37 \pm 2^\circ\text{C}$  for 24 h. After incubation, bacterial colonies with distinct morphological characteristics were selected and purified on LB agar plates by repeated streaking and stored at  $4^\circ\text{C}$  for further analysis.

For screening, the isolated strains were inoculated on LB agar plates containing 100 mg/L of azo dyes RR and RB and incubated at  $37^\circ\text{C}$  for 4 days. Based on the formation of the decolourization zone, they were selected for their colour removal efficiency in a synthetic medium containing 100 mg/L azo dyes. After incubation, aliquots of 7 mL broth were collected and centrifuged at 4000 rpm for 15 min. The absorbance (OD) of the supernatant was determined using a UV-Vis spectrophotometer (Model: Cyberlab UV-100, USA). The strains with the highest decolourizing abilities were subjected to further characterization. All tests were performed in triplicates. The formula used to calculate decolourization (%) is as follows:

$$\text{Decolorization (\%)} = \frac{\text{Abs}_{\text{initial}} - \text{Abs}_{\text{final}}}{\text{Abs}_{\text{initial}}} \times 100 \quad (1)$$

**Optimization of physio-chemical parameters:** The optimization of the culture conditions for enhanced decolourization of the azo dyes using the selected bacterial isolate *Bacillus* sp. (TDS50) was studied in 50 mL of LB broth amended with 100 mg/L of RR and RB followed by incubation in an orbital shaker with different carbon sources (glucose, sucrose and starch), temperatures (25, 30, 35, 40 and  $45^\circ\text{C}$ ), pH (5, 6, 7, 8 and 9) and inoculum concentrations (0.5, 0.75, 1.0, 1.25 and 1.5%) respectively. Periodically, the supernatant from each treatment was obtained and its colour was analyzed using a UV-Vis spectrophotometer.

**SEM analysis:** The bacterial biomass of TDS50 grown in LB broth containing azo dyes (RR and RB), was obtained and its morphological features were analyzed using a field emission scanning electron microscope (SEM) (Model: SEM-ZEISS, Germany). After drying using a critical point dryer, the samples were gold coated with platinum by an ion sputter coater (Quorum Technologies, U.K.).

## Production and characterization of extracellular metabolites

**Screening of bioflocculants (BF) and biosurfactants (BS) producing bacteria:** The agar plate enrichment method was used to screen the bacterial strains that produce BF. The composition of the growth media used in this study were as follows (g/L): glucose, 15; peptone, 10; yeast extract, 5; NaCl, 5 and agar, 20. Bacterial colonies were selected based on their unique morphology. The BF production medium were as follows (g/L): glucose, 10; peptone, 5; yeast extract 2.5;  $\text{K}_2\text{HPO}_4$ , 5 g/L;  $\text{KH}_2\text{PO}_4$ , 2;  $\text{MgSO}_4 \cdot 7\text{H}_2\text{O}$ , 0.2; and NaCl, 0.1. The flocculating activity of BF was assessed using the modified kaolin clay method after centrifuging the resulting culture broth [18]. The sample was prepared by adding 0.1 mL of cell-free supernatant, 0.9 mL of  $\text{CaCl}_2$  (1% w/w) and 9 mL of kaolin suspension (5 g/L) to form the assay mixture. After 5 min of vortexing, the mixture was left to stand for 10 min. The flocculation activity was calculated using the following eqn. 1:

$$\text{Flocculating activity} = \frac{A - B}{A} \times 100 \quad (2)$$

where A is the OD at 550 nm of the control sample and B is the OD at 550 nm of the test sample.

For subsequent analysis of its capacity to produce BS, the bacterial strain with the highest flocculating activity (TDS50) was chosen. Hemolytic activity was performed on blood agar supplemented with 5% (v/v) human blood, the bacterial strain TDS50 was inoculated and it was then incubated for 48 to 72 h at  $37^\circ\text{C}$  [19]. Hemolysis around the colonies on the plates, which indicates BS synthesis, was visually examined.

**Extraction and characterization of BF and BS:** The BF extraction and purification were done by the modified method of Cosa *et al.* [20]. The culture broth enhanced with TDS50 was incubated for 72 h and centrifuged at 4000 rpm for 30 min at  $4^\circ\text{C}$ . To eliminate the bacterial cells, the culture broth was diluted with an equal volume of distilled water and centrifuged

at 4000 rpm for 30 min. After discarding the pellet, two volumes of cold ethanol were added to the supernatant, which was then left to stand at 4 °C overnight to obtain a precipitate. Chloroform and *n*-butyl alcohol (5:5 v/v) were added to the solution while stirring and the mixture was allowed to stand at room temperature overnight. The supernatant was centrifuged again for 15 min at 4000 rpm at 4 °C and double the volumes of ethanol was added to obtain precipitate. The precipitates were then vacuum-dried and re-dissolved in distilled water to obtain pure BF [21].

Biosurfactants (BS) was extracted using a method previously described by Ibrahim [22]. The culture supernatants were acidified with 6 N HCl to a pH of 2.0 after centrifuging the bacteria at 6000 rpm for 15 min at 4 °C. The culture supernatant was added to the separating funnel and organic solvents namely methanol and chloroform (1:2, v/v) were added two times. The solvent mixtures with culture were then allowed to stand for phase separation, after which the organic phases were collected, evaporated to produce viscous yellowish products and dissolved in methanol.

**Surface activity of Biosurfactants (BS):** Surface activity of BS was measured using the oil spread assay and an emulsification index ( $E_{24}$ ). For the oil-spreading technique, 20 mL of distilled water was poured into a Petri dish (15 cm in diameter). Then, 15  $\mu$ L of engine oil was added to the surface of the water, followed by the addition of 10  $\mu$ L of supernatant to the oil surface. An oil-free clearing zone was formed when displaces the oil, it confirms the presence of BS. The activity of the BS in displacing the oil can be measured using the displacement activity, which can be determined by measuring the clearing zone. The diameter of the clear zone on the oil surface was measured and the time taken to achieve spread was noted [22].

The emulsification ability of BS was also evaluated using a previously described method [19]. For this method, 4 mL of fresh engine oil, used engine oil, kerosene, diesel and petrol were added to an equal volume of 4 mL of cell-free supernatant in a test tube. After vortexing for 5 min at a high speed, a mixture was left to ideal for approximately 24 h. Emulsification index ( $E_{24}$ ) was calculated using the following eqn. 2:

$$E_{24}(\%) = \frac{\text{Total height of emulsified layer}}{\text{Total height of liquid column}} \times 100 \quad (2)$$

**Stability evaluation of BF and BS:** Stability studies were performed using cell-free broth (crude BS) obtained by centrifuging the cultures at 5000 rpm for 20 min. The pH of BS (4 mL) was adjusted to 2, 4, 6, 8 and 10 using NaOH or HCl, after which  $E_{24}$  was determined. To evaluate the heat stability of the BS, the broth was heated to different temperatures (20, 30, 40, 50 and 60 °C) for 1 h and allowed to cool to room temperature.  $E_{24}$  was then determined to assess the BS heat stability [23].

**Dosage concentration of BF and BS:** The dosage concentration of purified BF was used to evaluate its effect on the flocculating activity [11]. A concentration range of 0.2-1.0 mg/mL of BF was prepared. The flocculation activity was calculated using previously described methods. Similarly, BS was prepared at the same concentration range from 0.2 to 1.0 mg/mL. Then,  $E_{24}$  was calculated using previously described methods and the values were measured.

**Determination of ionic character in BS and BF:** The agar double diffusion method was used to measure the ionic charges of the BS and BF. Two rows of wells were made with a low hardness agar (1% agarose) that were regularly spaced apart. A pure compound with a known ionic charge was placed in the wells in one row, whereas the BS or BF solution was placed in the wells of the other. The cationic compound selected was  $\text{BaCl}_2$  at 50 mM, whereas the anionic one was sodium dodecyl sulfate (SDS) at 20 mM. The mixture was kept at room temperature for 48 h. The ionic nature of BS and BF is indicated by the formation of precipitation lines between the wells [24].

**Chemical characteristics of BF and BS:** The BF and BS sugar contents were determined using phenol-sulfuric acid method, for which glucose was used as a standard [25] and the total protein content was determined using the Lowry method with bovine serum albumin (BSA) as standard [26]. The functional moieties within the molecules were identified using an FTIR analyzer. The samples were mixed with KBr, ground, fused into thin pellets and fixed in a sample holder in Shimadzu IRSpirit instrument used for the FTIR analysis in the range of 4000-400  $\text{cm}^{-1}$ .

**Removal of azo dyes from textile effluent using lab-scale bioreactor:** Bacterial treatment of textile wastewater was carried out using an aerobic bioreactor. The sample was collected from dyeing units in the Erode district, India and contained approximately 100 mg/L RR and RB. The treatment setup consisted of a reactor, reservoir, settling, filtration and collection tanks. The bioreactor setup was designed to remove the azo dyes RR and RB from contaminated wastewater following the wastewater treatment system proposed by Seenivasagan *et al.* [27]. All tanks were made up of tarson and have 10 L capacities. A total of 10 L of textile effluent containing 100 mg/L of dyes was placed in a reactor tank, subsequently, 1% glucose as a carbon source and 1 OD of inoculums were added. A mechanical stirrer was incorporated into the bioreactor setup to ensure that the microorganisms received nutrients uniformly. Every 12 h, 10 mL of the sample was collected from the reactor tank and centrifuged at 4000 rpm for 20 min and the dye removal efficiencies were analyzed using a UV-vis spectrophotometer at 515 and 600 nm. The pellet formed after centrifugation (4000 rpm for 20 min) was resuspended in 10 mL of distilled water and the absorbance at 600 nm was used to measure the bacterial cell growth.

**Degradation analysis of RR and RB azo dyes:** The decolourized broth was used to separate the metabolites using the solvent extraction method [28]. An equal volume of ethyl acetate was added to the decolourized broth to extract the metabolites. Anhydrous sodium sulfate was used to dehydrate the extracted metabolites and a rotary evaporator was used for drying. The FTIR analysis (Shimadzu IR Spirit) was also carried out. The degraded metabolites were identified using Shimadzu QP2020 gas chromatography coupled with mass spectroscopy.

**Application of BF and BS on dye removal:** Erlenmeyer flasks were used to study the BF and BS dye removal potentials. Approximately 100 mg/L solutions of RR and RB aqueous dye solutions were added, along with 200 ppm and 400 ppm BF and BS, respectively. The flasks were kept at an orbital shaker



at 200 rpm for 3 min and then the speed was reduced to 40 rpm for 5 min. Then, the flasks were left at room temperature for 10 min for sedimentation. Samples were collected every 10 min for 1 h. The absorbance was measured at 515 nm and 600 nm for RR and RB dyes, respectively, using a UV-vis spectrophotometer. The dye removal (%) was calculated using eqn. 3:

$$\text{Decolorization} = \frac{\text{Abs}_{\text{initial}} - \text{Abs}_{\text{final}}}{\text{Abs}_{\text{initial}}} \times 100 \quad (3)$$

**Phytotoxicity assay of treated textile effluent on seed germination of green gram:** The phytotoxicity of RR, RB and their degraded products was evaluated using a seed germination assay. The dye samples and their treated metabolites from the bioreactor were used for the study, including plain water as a control and a green gram (*Phaseolus aureus*) was evaluated at room temperature. The germination index (%), root length and shoot length were measured after 7 days.

**Statistical analysis:** All tests were performed in triplicates. The collected data from each set of experiments are expressed as the mean  $\pm$  standard deviation. The experimental data were analyzed using Origin software (Version 9.5).

## RESULTS AND DISCUSSION

### Isolation and screening of azo dye degrading bacteria:

Isolated bacterial strains were identified using Bergey's Manual of Determinative Bacteriology [29]. A total of 138 bacterial strains were isolated and identified based on their culture morphology, staining techniques, motility and various biochemical assays. The generic distribution of the isolates was recorded as 45% of *Bacillus* spp., 18% of *Listeria* spp., 14% of *Enterobacteriaceae*, 12% of *Micrococcus* spp., 8% of *Pseudomonas* spp., 2% of *Vibrio* spp. and 1% of *Aeromonas* spp.

All bacterial strains were subjected to primary screening to observe visible decolourization of the dyes. Among the strains, 69 showed degradation of RR dye and 56 showed degradation of RB. The remaining bacterial strains showed no efficiency in RR and RB degradation. Isolates that decolourized both the azo dyes were retained for secondary screening. Among the different isolates, the strain TDS50 (Fig. 1) showed the highest decolourization potential. The results showed that 97% degradation of RR and 96% degradation of RB at 100 mg/L concentration within 24 h under static conditions. However, the enzymatic degradation seemed to be the main mechanism for the test dye decolourization [30]. The potential dye degrader TDS50 was identified as *Bacillus* sp. and demonstrated that azo dyes bound to the cell wall of dye-decolourizing isolates were visible after centrifugation, as the bacterial pellets were red or blue.

**Optimization of the parameters on decolourization of RR and RB azo dyes:** Optimizing various culture conditions for the selected microorganisms can improve the decolourization process. The effects of various carbon sources on the decolourization of RR and RB dyes were studied and the results are shown in Fig. 2a. Among the carbon sources, glucose yields decolourization of approximately 96% of RR and 95% of RB. Sucrose showed a degradation yield of around 83% for RR and 75% for RB, while starch yielded 74% of RR and 62% of RB. Different carbon sources may have varying properties during

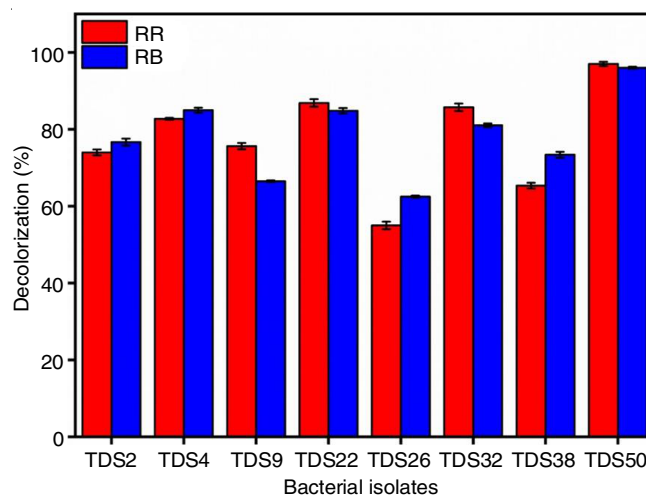


Fig. 1. Screening of dye-degrading bacteria

the decolourization process. During their regular growth cycle, bacteria use glucose as a carbon source, providing the biomass required for biodegradation [31]. For example, when xylose is present, only 25% decolourization of RR takes place, whereas sucrose can achieve 80% decolourization [32].

Temperature and initial pH of the medium are known to have a significant impact on biological decolourization [33]. Temperature plays a crucial role in microbial vitality and function and influences biochemical changes within microbial cells [34]. The decolourization efficiencies of RR and RB dyes at temperatures ranging from 25 °C to 45 °C were studied. Maximum decolourization of 96% and 97% was recorded in an aqueous medium containing RR and RB, respectively, at 35 °C. At 25 °C, 30 °C, 40 °C and 45 °C, 57%, 64%, 64% and 43% of decolourization was recorded for RR and 65%, 76%, 77% and 52%, respectively were recorded for RB (Fig. 2b). The overall activity of many enzyme-mediated processes leads to the development of microbes at various temperatures. Therefore, there is a strong correlation between the rate of microbial growth, enzyme activity and temperature [35]. Generally, higher temperatures lead to more development and activity, but extremely high or low temperatures cause these effects to decline abruptly and rapidly. This experiment revealed the same pattern: bacterial strains exhibited improved decolourization at 25 °C and 40 °C and were suppressed at 45 °C. A comparable results were found with methyl red; the decolourization was completely stopped at 45 °C and is effective between 27 °C and 37 °C [36].

Changes in the pH of the growth medium lead to changes in bacterial activity, growth rate and decolourization efficiency. At an appropriate pH range, bacteria become active. The optimal pH for growth is the same for dye decolourizing activity, as it is a primary metabolic process. The effect of pH in the range 5-9 on the decolourization of RR and RB dyes was studied (Fig. 2c). The maximum decolourization of 96% and 95% of RR and RB respectively was observed at pH 7. A relatively neutral pH usually promotes the azo dye bio-decolourization [30]. A progressive increase in decolourization was obtained from pH 6 to 7, followed by a decline up to pH 9. At pH 5, 6, 8 and 9, the decolourization percentages of RR were 47%, 55%, 73% and 54%, respectively. The decolourization of RB in the

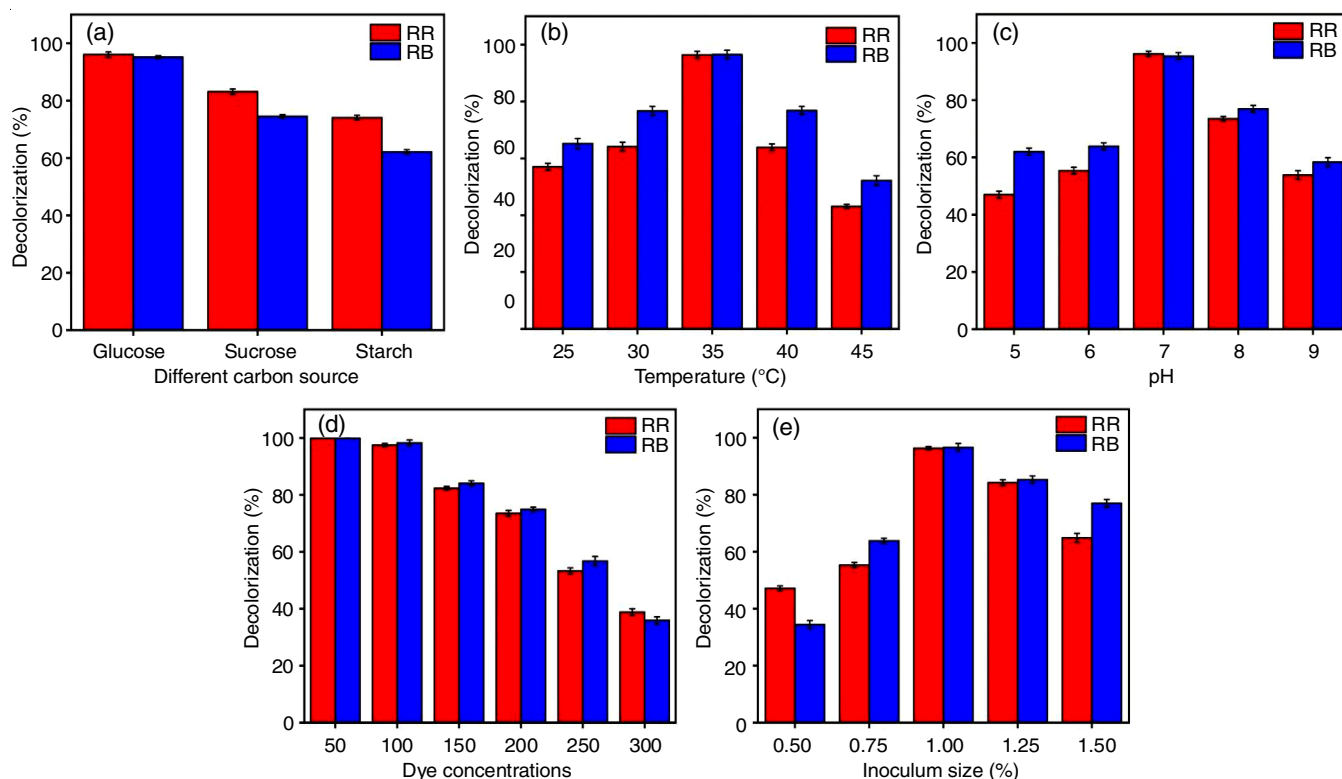


Fig. 2. Optimization of the parameters on decolorization. Different carbon source (a), temperature (b), pH (c), dye concentration (d), inoculum size (e)

medium at pH 5, 6, 8 and 9 was 62%, 63%, 76% and 58%, respectively. A higher pH level may result in a decrease in enzymatic and biological activity, which inhibits decolourization [37].

RR and RB dyes were decolourized at different concentrations (50-300 mg/L) and as the dye concentration increased, the ability of isolate TDS50 to decolourize RR and RB dyes decreased (Fig. 2d). A complete decolourization was obtained at 50 mg/L RR and RB after 24 h of incubation. The highest decolourization, 97% of RR and 98% of RB dye was obtained at 100 mg/L. At 300 mg/L, the isolate dye decolourization potential dropped significantly, reaching 39% of RR and 36% of RB. The efficiency of decolourization may be reduced at higher dye concentrations because of its potential to inhibit bacterial growth and metabolic activity [37]. The size of the inoculum was also crucial; in this case, different concentrations between 0.5 and 1.5% were tested and 1% of the inoculum was

used to achieve the maximum decolourization. As shown in Fig. 2e, the decolourization efficiency of dyes was approximately 96% for RR and 97% for RB.

**Effect of RR and RB azo dyes on bacterial cell morphology:** SEM analysis of the bacterial strain TDS50 grown in LB broth (with and without RR and RB dye) during the degradation process is presented in Fig. 3. The bacterial cells grown in LB broth without the dye (control) had a smooth surface and were large and rod-shaped (Fig. 3a). In contrast, the bacterial cells grown in LB broth containing RR and RB dyes had a surface that was smaller, rougher, wrinkled and coagulated (Figs. 3b and c). Stress circumstances and dye deposited on the bacterial cell surface may have caused changes in the cell morphology of the bacterial cell surface [38].

**Screening of BF and BS-producing bacteria:** Eight potential dye degraders were screened for use in BF production.

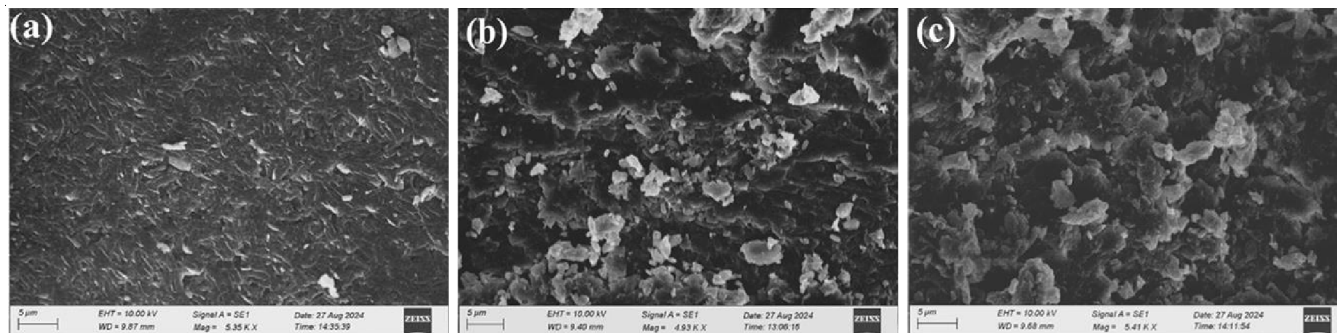


Fig. 3. SEM analysis of bacterium TDS50 grown in LB broth containing azo dyes. Bacterium grown in LB broth without dye (a), Bacterium grown in LB broth with RR (b) and Bacterium grown in LB broth with RB (c)

Four isolates from this sample showed mucoid, ropy and glistening colonies. Flocculating activity was also examined. Compared to other strains, the potential dye degrader TDS50 showed higher flocculating activity of 75.26% in this instance (Fig. 4a), therefore, it was further investigated. The strain TDS50 culture supernatant showed a  $\beta$ -hemolytic pattern, it results in complete lysis of red blood cells. The bacterial strains ability to produce BS was associated with the hemolytic zones. Blood agar hemolysis is a major screening technique because of the connection between hemolytic activity and BS production [39].

#### Properties of BS produced by TDS50

**Surface activity of BS:** The surface activity of the surfactant containing solution at the oil-water interface was measured using the oil-spreading technique [22]. The strain TDS50 produced a BS, resulting in a clear zone 33 mm in diameter in the liquid medium, confirming the presence of BS in the cell-free culture broth. The cell-free supernatant containing BS was tested for its ability to emulsify two immiscible liquids into a single, transparent emulsified layer by  $E_{24}$  [40]. The cell-free supernatant of strain TDS50 is emulsified with fresh engine oil, used engine oil, kerosene, diesel and petrol. The diesel oil, fresh engine oil and used engine oil were effectively emulsified by

the strain TDS50 (Fig. 4b). In contrast, they failed to emulsify kerosene and petrol, which may be due to the lower molecular weights of these compounds [41]. The highest  $E_{24}$  value for the strain TDS50 was 77% for used engine oil.

**Stability nature of BS:** The stability of BS under harsh operating and environmental conditions, such as temperature and pH, determines their use in a variety of applications. According to the  $E_{24}$  values derived from the stability studies of the BS, which are shown in Fig. 4c, they maintained their activity throughout the temperature range under study (20-60 °C), with somewhat greater activity of 76.6% emulsification activity at 50 °C. The BS application can be affected by its stability over a range of pH values. The BS activity was assessed in a pH ranges of 2-10. At pH 8, the maximum emulsification activity of 62.5% was attained (Fig. 4d).

#### Physio-chemical properties of BF and BS

**Dosage concentration of BF and BS:** Excessive and inadequate dosages may result in the inhibition or a decrease in flocculation. The BF dosage and flocculating activity were studied and the results are shown in Fig. 5a. A dosage of 0.2% showed the highest flocculating activity of 69% compared to other concentrations. The dosage concentration of BS was

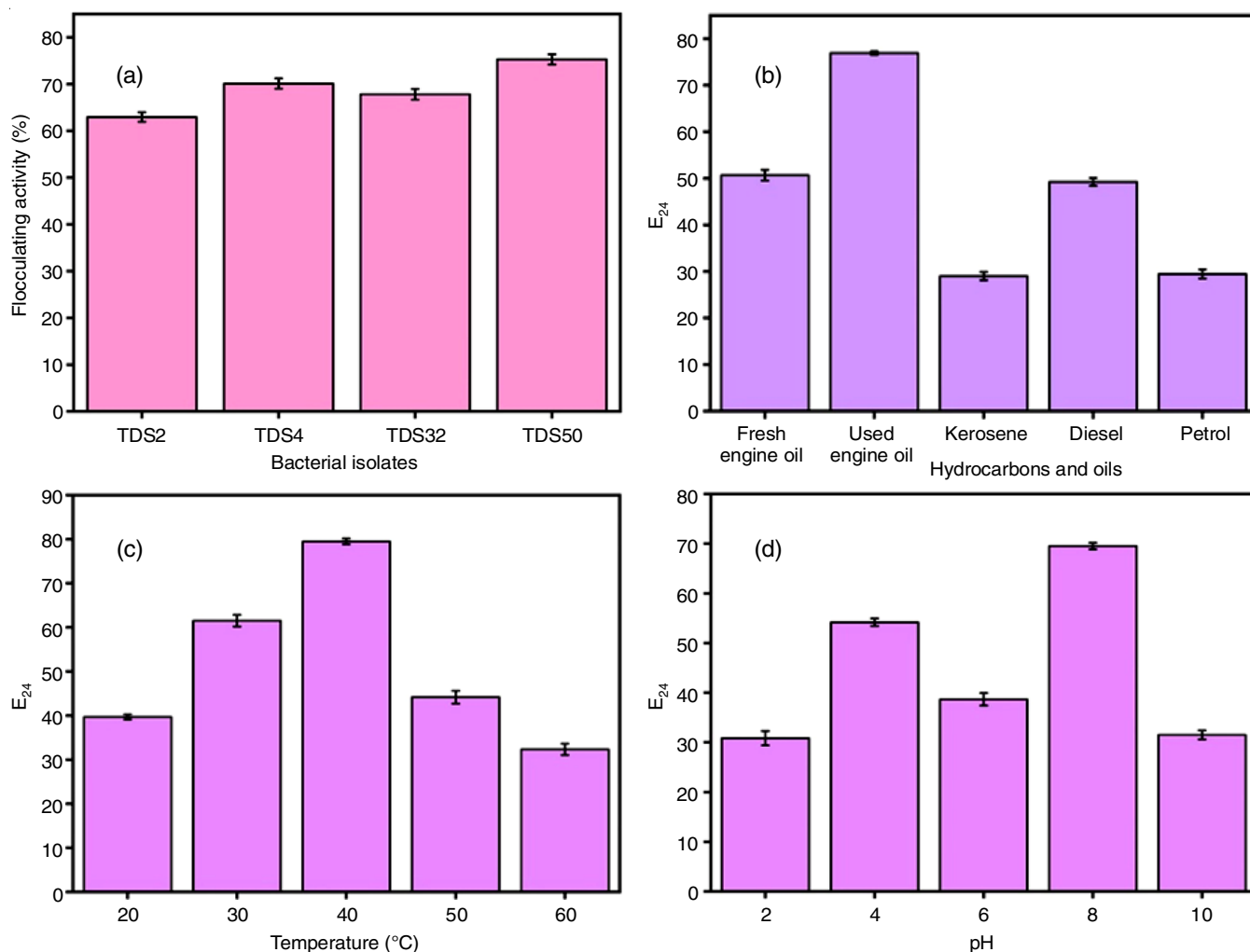


Fig. 4. Screening of BF-producing bacteria (a) and BS-producing bacteria (b), Stability studies of BS under different Temperature (c), pH (d)

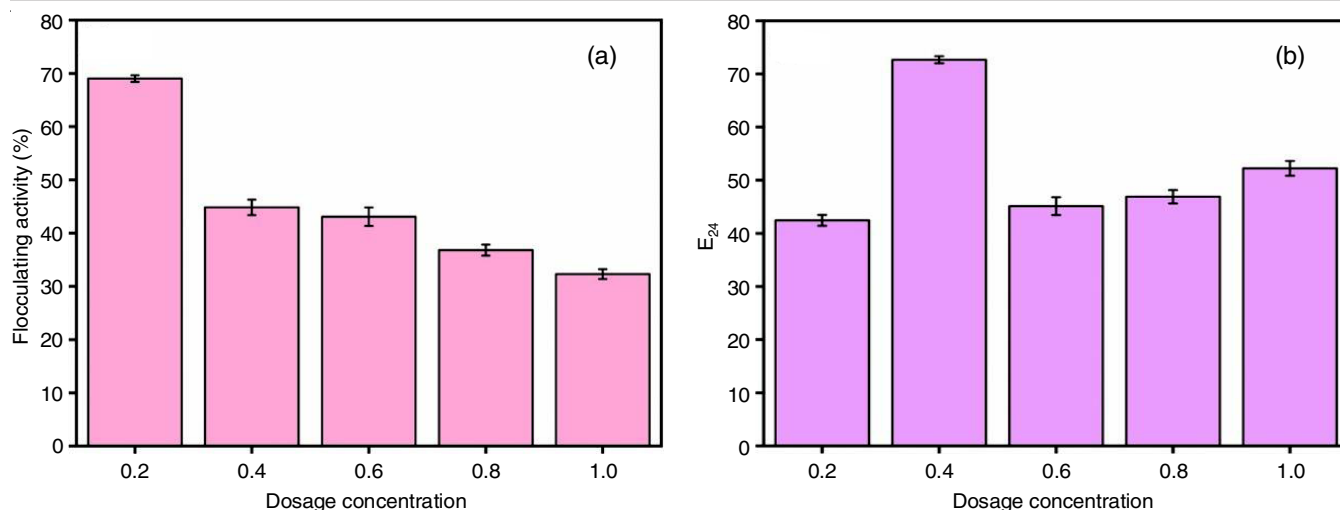


Fig. 5. Dosage concentration of BF (a) and BS (b)

studied by measuring the  $E_{24}$  values. In this case, a dosage of 0.4 mg/mL showed the highest  $E_{24}$  index values at 72% (Fig. 5b).

**Ionic characteristics of BF and BS:** The ionic charges of BS and BF were determined using the agar double diffusion method. In this method, it showed a precipitation line between BS and the cationic compound barium chloride, indicating that BS is anionic. In contrast, precipitation lines were formed between the anionic compounds SDS and BF. The results observed in this study indicate the non-ionic nature of BF.

**Chemical components in the purified BF and BS:** The carbohydrate content in the BF and BS was estimated using the phenol-sulfuric acid method. The BF and BS contained 15% and 82% carbohydrates, respectively. The total protein content in the BF and BS was estimated using the Lowry method. The BF and BS had 27% and 70% protein contents, respectively. Compared to BF, BS had the highest amounts of carbohydrates and proteins.

**FTIR analysis of purified BF and BS:** BF showed a peak at  $3410.29\text{ cm}^{-1}$ , which represents the -OH group. The =CH stretching of the peaks was observed between  $2906.77\text{ cm}^{-1}$

and  $2856.23\text{ cm}^{-1}$  [42]. The peak at  $2395.48\text{ cm}^{-1}$  have been attributed to the amine group or  $\text{CO}_2$  adsorption [43]. The peak at  $1691.72\text{ cm}^{-1}$  and  $1636.64\text{ cm}^{-1}$  corresponds to the protein-specific C=O stretching and N-H bending [44]. The peak at  $1542.68\text{ cm}^{-1}$  represents the stretching of  $\text{NO}_2$  and  $1099.43\text{ cm}^{-1}$  corresponds to the -COO group of carboxylate ions in BF, which is stretched asymmetrically by C=O. The peaks at  $685.33\text{ cm}^{-1}$  and  $592.02\text{ cm}^{-1}$  represent the C=C bending and C-Cl stretching, respectively. The presence of these functional groups enhances the bioflocculant activity (Fig. 6a) [45].

BS showed peaks at  $2930.68\text{ cm}^{-1}$  and  $2860.68\text{ cm}^{-1}$ , representing the -CH<sub>2</sub>- stretching and -CH<sub>3</sub> stretching of the acyl chain [22]. The peaks at positions  $1653.10$ ,  $1239.74$  and  $1049.01\text{ cm}^{-1}$  correspond to the stretching of C=O, C-O and C-N and a distinct peak at  $1532.60\text{ cm}^{-1}$  represents an N-H band [46]. The band observed at peak  $1453.60\text{ cm}^{-1}$  corresponds to the aliphatic chain of the C-H group. Since all the functional groups are present, it is evident that the BS is a polypeptide (Fig. 6b).

**Bioreactor study on azo dye degradation:** Optimized levels of glucose and inoculum concentrations were incorporated into the bioreactor. The decolourization efficiency of dyes

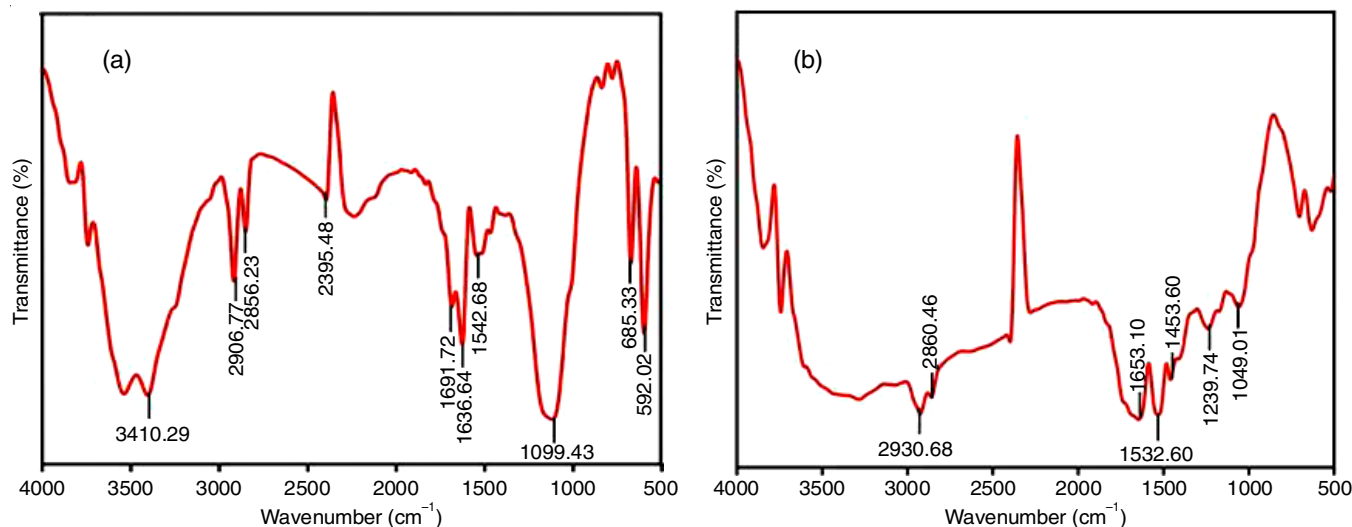


Fig. 6. FTIR analysis of BF (a) and BS (b)



RR and RB and the growth of the bacteria were studied for 10 days. The decolourization efficiency of the strain TDS50 was achieved as 98.30% for RR and 98.02% for RB. In the bioreactor approach, a control without inoculum was also maintained for the dyes RR and RB and their decolourization efficiency and cell growth were calculated for 10 days for the comparative study. The decolourization of the control was 39.32% for RR and 26.05% for RB. Figs. 7a and 7b show the RR decolourization removal rate and cell growth, respectively. The decolourization percentage rate of RB dye and their cell growth are shown in Figs. 7c and 7d.

#### FTIR characterization of treated and untreated water:

The FTIR spectra of the treated and untreated RR and RB dyes are shown in Fig. 8. The large, intense peak at  $3475.09\text{ cm}^{-1}$  for the untreated RR dye represents the -NH group. Other significant peaks include  $2894.76\text{ cm}^{-1}$  for  $-\text{CH}_2$  stretching,  $2355.51\text{ cm}^{-1}$  for  $\text{CO}_2$  stretching,  $1634.34\text{ cm}^{-1}$  for  $-\text{N}=\text{N}-$  stretching of azo bonds and  $1486.32\text{ cm}^{-1}$  for CH deformation. The peaks at  $1137.47\text{ cm}^{-1}$  for the  $-\text{C}-\text{OH}$  stretching of the secondary alcohol,  $1031.19\text{ cm}^{-1}$  for the  $-\text{S}=\text{O}$  stretching of sulfonic acid and  $621.04\text{ cm}^{-1}$  for the C-Cl stretching vibration (Fig. 8a).

The treated dyes show peaks at  $3268.02\text{ cm}^{-1}$  for O-H stretching of alcohol,  $2351.27\text{ cm}^{-1}$  stretching of carbon dioxide and  $1643.37\text{ cm}^{-1}$  for  $\text{C}=\text{O}$  stretching and  $1545.12\text{ cm}^{-1}$  represents the -N-O stretching of the nitro compound. The peaks at  $1389.62$ ,  $1044.78$  and  $514.51\text{ cm}^{-1}$  correspond to the C-H deformation, C-F stretching and C-I stretching, respectively. The bacterial breakdown of the azo bond breakage is indicated by the disappearance of the peak at  $1634.34\text{ cm}^{-1}$  (Fig. 8b).

The FTIR spectrum of untreated the RB dye showed an absorption peak at  $3487.82\text{ cm}^{-1}$  corresponding to the -NH azo bond group [38] (Fig. 8c). The peaks at  $3305.60\text{ cm}^{-1}$  indicate the presence of the -OH group and at  $2885.20\text{ cm}^{-1}$  represent the  $-\text{CH}_2$  stretching of the alkane group. The peak at  $2350.20\text{ cm}^{-1}$  shows a strong  $\text{O}=\text{C}=\text{O}$  stretching of carbon dioxide,  $1667.30\text{ cm}^{-1}$  for  $\text{C}=\text{N}$  stretching,  $1471.13\text{ cm}^{-1}$  and  $1137.07\text{ cm}^{-1}$  peaks represent C-H and  $-\text{SO}_2$  bending [47,48]. The peaks ranging from  $699$  to  $900\text{ cm}^{-1}$  represent C-H stretching peaks. In contrast, the treated RB showed different peaks compared to the untreated dye. The -OH and -NH peaks were shifted to  $3294.93\text{ cm}^{-1}$  and  $2952.66\text{ cm}^{-1}$ . The strong  $\text{O}=\text{C}=\text{O}$  stretching of carbon dioxide occurred in the peak position  $2350.20\text{ cm}^{-1}$ .

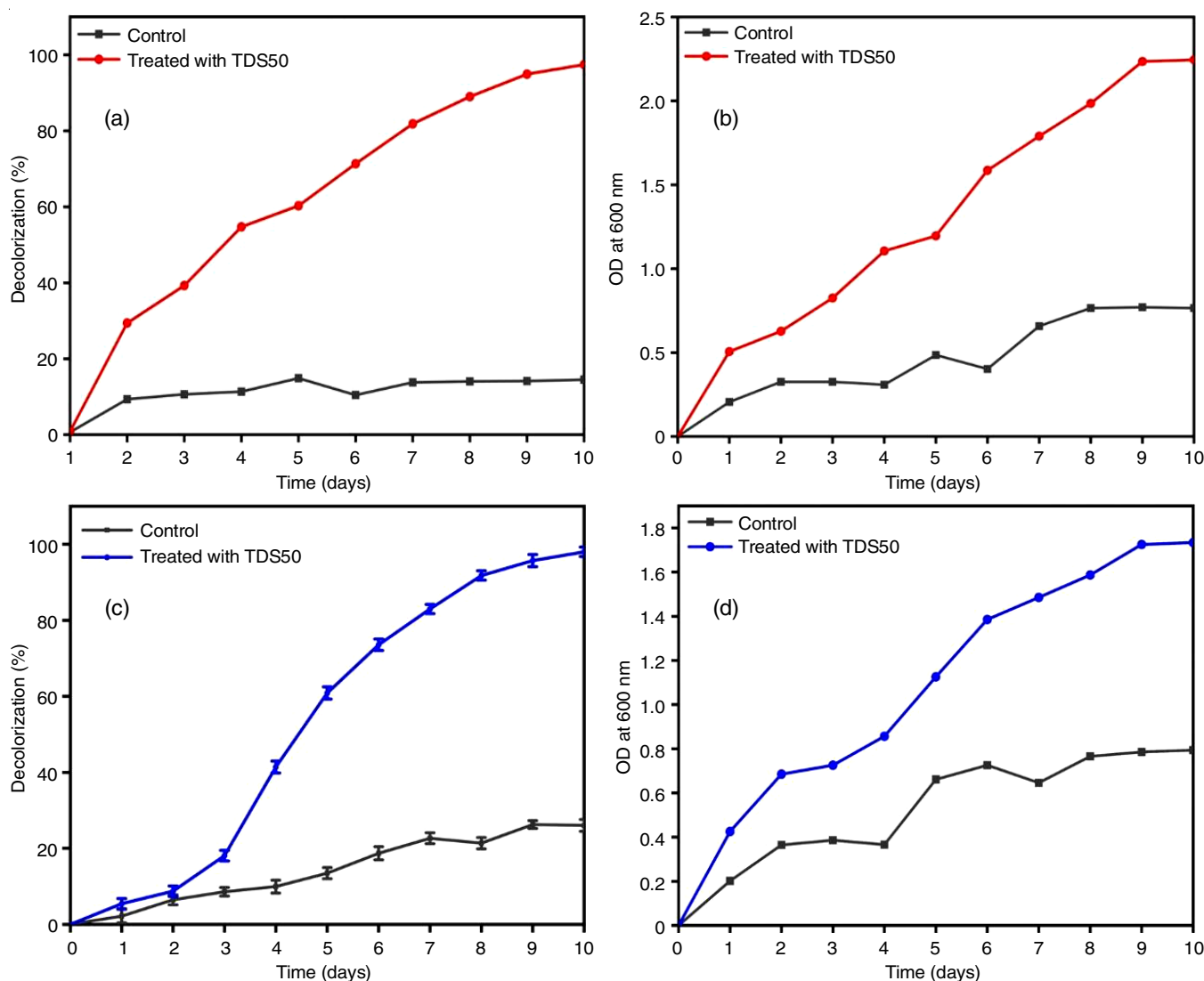


Fig. 7. Bioreactor treatment of RR (a&b) and RB (c&d) for decolorization removal rate and cell growth



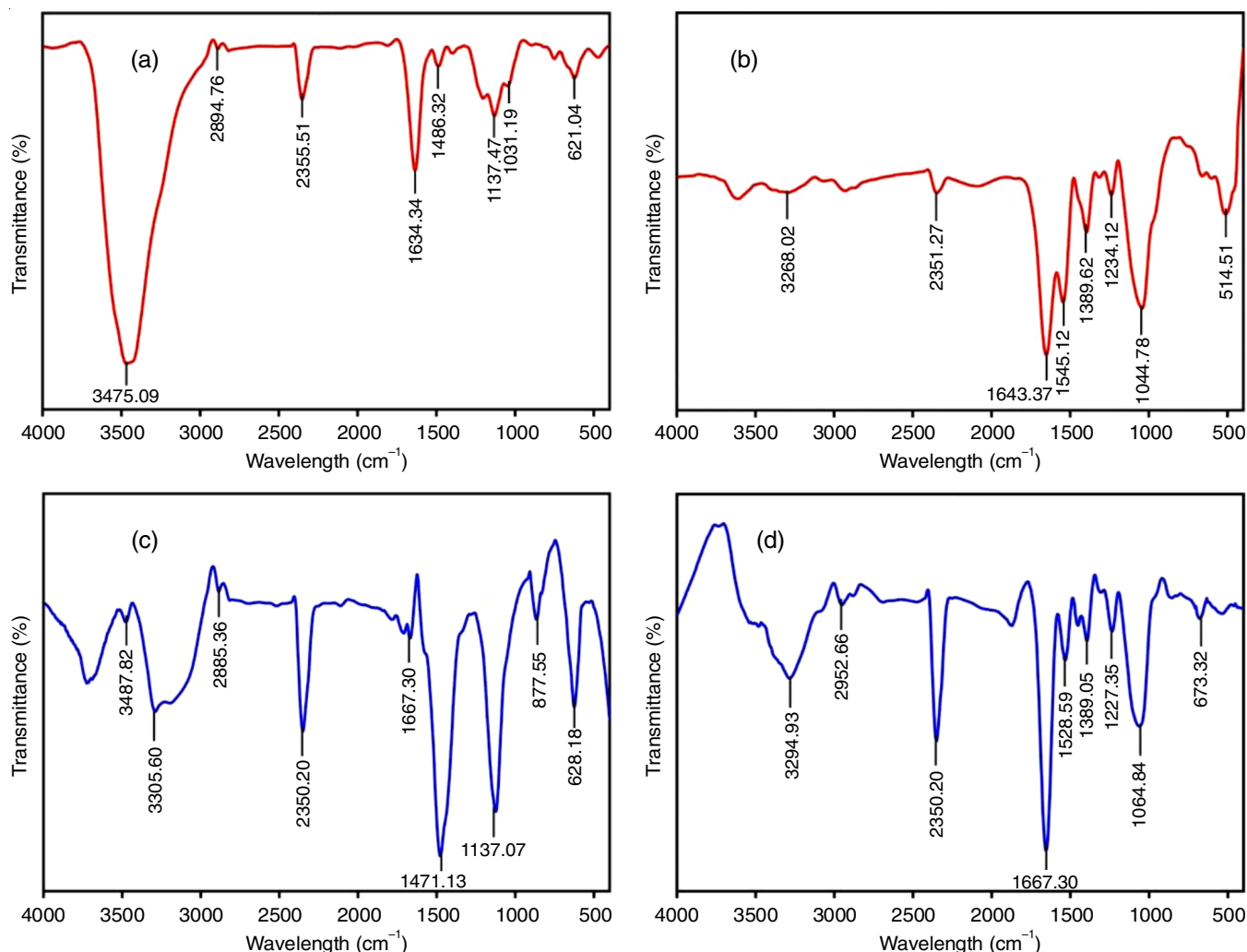


Fig. 8. FT-IR spectrum of untreated RR (a), treated RB dye (b), untreated RB (c) and treated RB (d) by an isolated bacterium

The peak at  $1667.30\text{ cm}^{-1}$  indicates the presence of  $\text{C}=\text{N}$ . The new peaks at  $1528.59$ ,  $1389.05$  and  $1227.35\text{ cm}^{-1}$  indicate the  $\text{N}-\text{O}$ ,  $\text{S}=\text{O}$  and  $\text{C}-\text{N}$  stretching, respectively. The peaks at  $1064.84\text{ cm}^{-1}$  for  $\text{C}-\text{O}$  stretching of the primary alcohol and  $673.32\text{ cm}^{-1}$  for  $\text{C}-\text{I}$  stretching. In treated samples, the azo bond cleavage is indicated by the disappearance of peak at  $3487.82\text{ cm}^{-1}$ . In this study, it is evident that certain peaks have disappeared entirely, some were changed and some new peaks emerged when compared to the untreated dye, indicating that the isolated bacterium degraded the RB azo dye, as shown in Fig. 8d.

**GC-MS characterization of treated and untreated water:** The GC-MS analysis was used to analyze the degraded metabolites formed from the bacterial-treated azo dyes. The compounds in the treated RR and RB samples are listed in Tables 1 and 2, respectively. The major peaks observed in the RR samples were 13.594, 17.530, 18.278, 20.427, 22.483, 23.823, 25.927 and 27.815, indicating the presence of hycanthone, dithiocarbamate, S-methyl-, N-(2-methyl-3-oxobutyl), methoxyacetic acid, 3-tridecyl ester, O-decylhydroxylamine, nitrobenzene, 1-iodo-2-methylundecane, triethylene glycol monododecyl ether, *bis*(2-Ethylhexyl) phthalate respectively (Fig. 9a). The peaks observed after RB degradation are 13.589, 17.164, 17.753, 18.169, 18.96, 20.4 and 20.659, indicating

the presence of d-Mannose, 1-deoxy-d-mannitol, octaethylene glycol monododecyl ether, d-glycero-d-galacto-heptose, hexaethylene glycol monododecyl ether, nitrobenzene and *bis*(2-ethylhexyl) phthalate respectively (Fig. 9b).

It is often recognized that dyes can have allergic, genotoxic, cytotoxic, carcinogenic and mutagenic effects in plants, fish, bacteria, mollusks and animals [28,49]. The decrease in dissolved oxygen content and the diminished ability of sunlight to penetrate seriously affect aquatic life [50,51]. Phthalates, such as *bis*(2-ethylhexyl) phthalate, were present in both treated dye samples, which are used in the textile manufacturing process printing stage as printing inks and adhesive additives. The presence of several aromatic compounds indicated the breakdown of the azo dye into simpler products.

**Application of BF and BS on azo dye removal:** The BF and BS on dye removal efficiencies were studied for the RR and RB dyes. In this, the  $0.2\text{ mg/mL}$  of BF decolourized RR up to 97.74% and RB at a rate of 98.04% after 60 min, as shown in Fig. 10a. BS in a  $0.4\text{ mg/mL}$  range had decolourized RR up to 96.79% and RB at 97.28% after 60 min, as shown in Fig. 10b.

**Phytotoxicity assay of treated textile effluent on seed germination of green gram:** Seed germination and plant

TABLE-1  
GC-MS SPECTRAL DATASHEET OF COMPOUNDS FORMED AFTER DEGRADATION OF REACTIVE RED (RR)

S. No.	Retention time (min)	m.w.	Name of the compound	m.f.	Compound structure
1	13.594	356	Hycanthone	$C_{20}H_{24}N_2O_2S$	
2	17.530	191	Dithiocarbamat, S-methyl-, N-(2-methyl-3-oxobutyl)	$C_7H_{13}NOS_2$	
3	18.278	272	Methoxyacetic acid, 3-tridecyl ester	$C_{16}H_{32}O_3$	
4	20.427	173	O-Decylhydroxylamine	$C_{10}H_{23}NO$	
5	22.483	123	Nitrobenzene	$C_6H_5NO_2$	
6	23.823	296	1-Iodo-2-methylundecane	$C_{12}H_{25}I$	
7	25.927	318	Triethylene glycol monododecyl ether	$C_{18}H_{38}O_4$	
8	27.815	390	Bis(2-Ethylhexyl) phthalate	$C_{24}H_{38}O_4$	

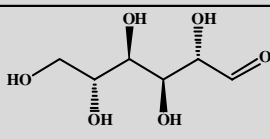
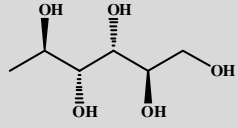
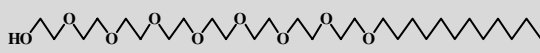
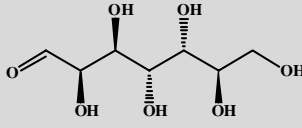
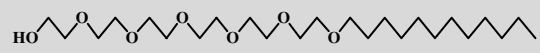
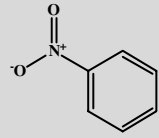
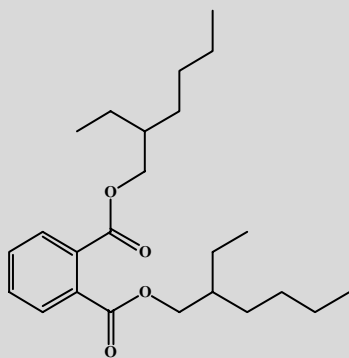
growth bioassays are the most widely used methods for evaluating the phytotoxicity of toxicants [52]. The growth of the roots and shoots of the green gram (*Phaseolus aureus*) was calculated after 7 days. The results revealed that the treated bacterial effluents from the bioreactor samples were non-toxic to plant growth. Thus, phytotoxicity experiments showed that the bacterial strain *Bacillus* sp. TDS50 has the potential to decolourize RR and RB. The study also found that raw and untreated textile dyes are toxic to plant growth. The results are presented in Table-3.

## Conclusion

The dye-degrading bacterium *Bacillus* sp. TDS50 was isolated from the textile industry effluent. The strain TDS50 has the potential to decolourize the RR and RB dyes. The opti-

mum conditions for decolourization of azo dyes were found to be glucose as a carbon source, pH 7 and temperature 35 °C for both the azo dyes. This study also examined the synthesis and extraction of bioflocuants (BF) and biosurfactants (BS) and their application in the removal of RR and RB dyes. FTIR analysis confirmed the presence of different functional groups in the BF and BS. Both the azo dyes RR and RB were greatly degraded by the selected bacterium TDS50 in the bioreactor under optimized conditions. The FTIR and GC-MS results also indicated the promising ability of the bacterial species TDS50 to produce significant microbial degradation of the azo dyes RR and RB. The phytotoxicity study showed that the breakdown products of RR and RB were non-toxic when compared to the parent dye. The current investigation highlights the effectiveness of the adopted strains in bioremediation.

TABLE-2  
GC-MS SPECTRAL DATASHEET OF COMPOUNDS FORMED AFTER DEGRADATION OF REACTIVE BLUE (RB)

S. No.	Retention time (min)	m.w.	Name of the compound	m.f.	Compound structure
1	13.589	180	d-Mannose	$C_6H_{12}O_6$	
2	17.164	166	1-Deoxy-d-mannitol	$C_6H_{14}O_5$	
3	17.753	538	Octaethylene glycol monododecyl ether	$C_{28}H_{58}O_9$	
4	18.169	210	d-Glycero-d-galacto-heptose	$C_7H_{14}O_7$	
5	18.96	450	Hexaethylene glycol monododecyl ether	$C_{24}H_{50}O_7$	
6	20.4	123	Nitrobenzene	$C_6H_5NO_2$	
7	20.659	390	Bis(2-ethylhexyl) phthalate	$C_{24}H_{38}O_4$	

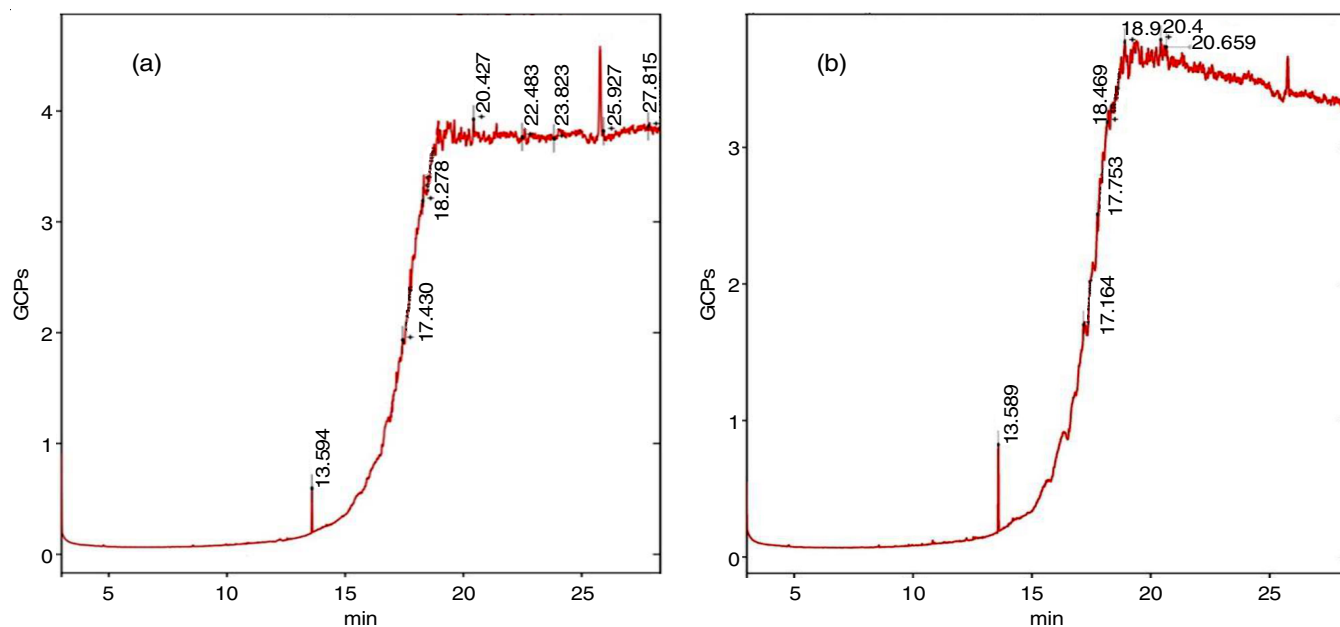


Fig. 9. GC-MS analysis of RR (a) and RB (b)

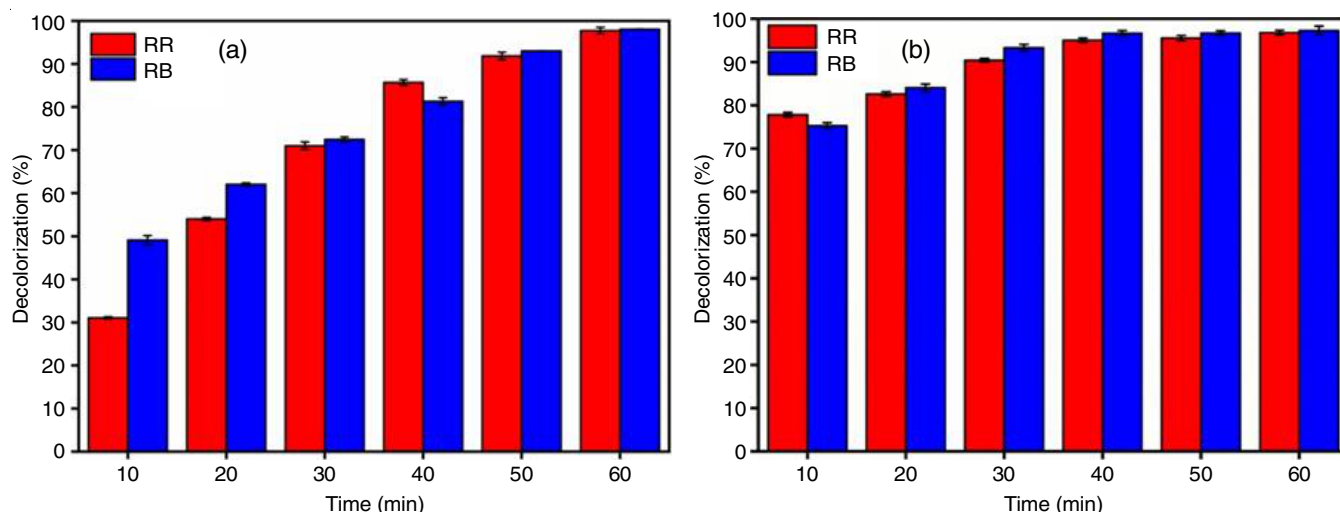


Fig. 10. Application of BF (a) and BS (b) on removal of azo dyes in synthetic medium

TABLE-3  
PHYTOTOXICITY OF TREATED AND UNTREATED RR AND RB ON *Phaseolus aureus*

Parameters	Distilled water	Untreated RR	Treated RR	Untreated RB	Treated RB
Seed germination (%)	100	80	100	37.5	100
Shoot length (cm)	14.16 ± 0.76	5.06 ± 0.90	11 ± 0.91	5.26 ± 0.64	12.6 ± 0.52
Root length (cm)	2.66 ± 0.41	1 ± 0.43	2.53 ± 0.55	0.78 ± 0.27	2.3 ± 0.45

### ACKNOWLEDGEMENTS

The Department of Microbiology, Periyar University, Salem, India, provided laboratory facilities for the entire research and instrumental support under DST-FIST (Ref No. SR/FST/LSI-640/2015(c)Dt.30/05/2016) is sincerely acknowledged.

### CONFLICT OF INTEREST

The authors declare that there is no conflict of interests regarding the publication of this article.

### REFERENCES

- X. Wang, F. Aulenta, S. Puig, A. Esteve-Núñez, Y. He, Y. Mu and K. Rabaey, *Environ. Sci. Ecotechnol.*, **1**, 100013 (2020); <https://doi.org/10.1016/j.ese.2020.100013>
- S. Benkhaya, S. M'rabet and A. El Harfi, *Heliyon*, **6**, e03271 (2020); <https://doi.org/10.1016/j.heliyon.2020.e03271>
- D. Prato-García, F.J. Cervantes and G. Buitrón, *J. Hazard. Mater.*, **250-251**, 462 (2013); <https://doi.org/10.1016/j.jhazmat.2013.02.025>
- R. Al-Tohamy, J. Sun, M.F. Fareed, E.R. Kenawy and S.S. Ali, *Sci. Rep.*, **10**, 12370 (2020); <https://doi.org/10.1038/s41598-020-69304-4>
- B. Lellis, C.Z. Fávoro-Polonio, J.A. Pamphile and J.C. Polonio, *Biotechnol. Res. Innov.*, **3**, 275 (2019); <https://doi.org/10.1016/j.biori.2019.09.001>
- A.C.R. Ngo and D. Tischler, *Int. J. Environ. Res. Public Health*, **19**, 4740 (2022); <https://doi.org/10.3390/ijerph19084740>
- L.D. Ardila-Leal, R.A. Poutou-Piñales, A.M. Pedroza-Rodríguez and B.E. Quevedo-Hidalgo, *Molecules*, **26**, 3813 (2021); <https://doi.org/10.3390/molecules26133813>
- E. Akceylan, M. Bahadır and M. Yılmaz, *J. Hazard. Mater.*, **162**, 960 (2009); <https://doi.org/10.1016/j.jhazmat.2008.05.127>
- X. Meng, G. Liu, J. Zhou and Q.S. Fu, *Bioresour. Technol.*, **151**, 63 (2014); <https://doi.org/10.1016/j.biortech.2013.09.131>
- M. Solís, A. Solís, H.I. Pérez, N. Manjarrez and M. Flores, *Process Biochem.*, **47**, 1723 (2012); <https://doi.org/10.1016/j.procbio.2012.08.014>
- P.H. Tsilo, A.K. Basson, Z.G. Ntombela, T.S. Maliehe and V.R. Pullabhotla, *Int. J. Environ. Res. Public Health*, **19**, 3148 (2022); <https://doi.org/10.3390/ijerph19063148>
- G.P. Sheng, H.Q. Yu and X.Y. Li, *Biotechnol. Adv.*, **28**, 882 (2010); <https://doi.org/10.1016/j.biotechadv.2010.08.001>
- J.C. Mata-Sandoval, J. Karns and A. Torrents, *Environ. Sci. Technol.*, **34**, 4923 (2000); <https://doi.org/10.1021/es0011111>
- S.Y. Chen, W.B. Lu, Y.H. Wei, W.M. Chen and J.S. Chang, *Biotechnol. Prog.*, **23**, 661 (2007); <https://doi.org/10.1021/bp0700152>
- I. Mnif and D. Ghribi, *World J. Microbiol. Biotechnol.*, **31**, 1001 (2015); <https://doi.org/10.1007/s11274-015-1866-6>
- C. Nikolova and T. Gutierrez, *Front. Bioeng. Biotechnol.*, **9**, 626639 (2021); <https://doi.org/10.3389/fbioe.2021.626639>
- S. Gaur, S. Gupta and A. Jain, *Bioremediat. J.*, **25**, 308 (2021); <https://doi.org/10.1080/10889868.2020.1871316>
- S. Bala Subramanian, S. Yan, R.D. Tyagi and R.Y. Surampalli, *Water Res.*, **44**, 2253 (2010); <https://doi.org/10.1016/j.watres.2009.12.046>
- S. Nor, A. Abdullah, A. Yuniarto, Z. Ibrahim, M.H.M. Nor and T. Hadibarata, *Environ. Technol. Innov.*, **22**, 101533 (2021); <https://doi.org/10.1016/j.eti.2021.101533>
- S. Cosa, A.M. Ugbenyen, L.V. Mabinya, K. Rumbold and A.I. Okoh, *Environ. Technol.*, **34**, 2671 (2013); <https://doi.org/10.1080/09593330.2013.786104>
- O. Li, C. Lu, A. Liu, L. Zhu, P.M. Wang, C.D. Qian, X.H. Jiang and X.C. Wu, *Bioresour. Technol.*, **134**, 87 (2013); <https://doi.org/10.1016/j.biortech.2013.02.013>
- H.M. Ibrahim, *Egypt. J. Pet.*, **27**, 21 (2018); <https://doi.org/10.1016/j.ejpe.2016.12.005>
- O.S. Obayori, M.O. Ilori, S.A. Adebuseye, G.O. Oyetibo, A.E. Omotayo and O.O. Amund, *World J. Microbiol. Biotechnol.*, **25**, 1615 (2009); <https://doi.org/10.1007/s11274-009-0053-z>



24. R.D. Rufino, J.M. de Luna, G.M. de Campos Takaki and L.A. Sarubbo, *Electron. J. Biotechnol.*, **17**, 34 (2014);  
<https://doi.org/10.1016/j.ejbt.2013.12.006>
25. M.F. Chaplin, Carbohydrate analysis. (2006);  
<https://doi.org/10.1002/3527600906.mcb.200300011>
26. O.H. Lowry, N.J. Rosebrough, A.L. Farr and R.J. Randall, *J. Biol. Chem.*, **193**, 265 (1951);  
[https://doi.org/10.1016/S0021-9258\(19\)52451-6](https://doi.org/10.1016/S0021-9258(19)52451-6)
27. R. Seenivasagan, P. Ayyasamy, R. Kasimani, A. Karthika, S. Rajakumar, O.O. Babalola, in eds.: M. Prashanthi, R. Sundaram, A. Jeyaseelan and T. Kaliannan, Nitrate Removal from Ground Water Through Lab Scale Bioreactor using Dissimilatory Nitrate Reducer *Bacillus weihenstephanensis* (DS45), In: Bioremediation and Sustainable Technologies for Cleaner Environment. Environmental Science and Engineering, Springer, Cham. pp 79–94 (2017).
28. V.V. Dawkar, U.U. Jadhav, S.U. Jadhav and S.P. Govindwar, *J. Appl. Microbiol.*, **105**, 14 (2008);  
<https://doi.org/10.1111/j.1365-2672.2008.03738.x>
29. D.H. Bergey, Bergey's Manual of Determinative Bacteriology, Williams & Wilkins Co.: Baltimore, USA (2000).
30. P.K. Chukowry, A. Mudhoo and S.J. Santchurn, *Environ. Chem. Lett.*, **15**, 531 (2017);  
<https://doi.org/10.1007/s10311-017-0627-1>
31. N. Bhatt, K.C. Patel, H. Keharia and D. Madamwar, *J. Basic Microbiol.*, **45**, 407 (2005);  
<https://doi.org/10.1002/jobm.200410504>
32. H.A. Modi, G. Rajput and C. Ambasana, *Bioresour. Technol.*, **101**, 6580 (2010);  
<https://doi.org/10.1016/j.biortech.2010.03.067>
33. X. Xiao, C.C. Xu, Y.M. Wu, P.J. Cai, W.W. Li, D.L. Du and H.Q. Yu, *Bioresour. Technol.*, **110**, 86 (2012);  
<https://doi.org/10.1016/j.biortech.2012.01.099>
34. R.G. Saratale, G.D. Saratale, J.S. Chang and S.P. Govindwar, *J. Taiwan Inst. Chem. Eng.*, **42**, 138 (2011);  
<https://doi.org/10.1016/j.jtice.2010.06.006>
35. C.I. Pearce, J.R. Lloyd, J.T. Guthrie, *Dyes Pigm.*, **58**, 179 (2003);  
[https://doi.org/10.1016/S0143-7208\(03\)00064-0](https://doi.org/10.1016/S0143-7208(03)00064-0)
36. P.K. Wong and P.Y. Yuen, *Water Res.*, **30**, 1736 (1996);  
[https://doi.org/10.1016/0043-1354\(96\)00067-X](https://doi.org/10.1016/0043-1354(96)00067-X)
37. A.V. Bunti'c, M.D. Pavlovi'c, D.G. Antonovi'c, S.S. Šiler-Marinković and S.I. Dimitrijević-Branković, *J. Clean. Prod.*, **148**, 347 (2017);  
<https://doi.org/10.1016/j.jclepro.2017.01.164>
38. R. Kishor, D. Purchase, G.D. Saratale, R.G. Saratale, L.F.R. Ferreira, M. Bilal, R. Chandra and R.N. Bharagava, *J. Environ. Chem. Eng.*, **9**, 105012 (2021);  
<https://doi.org/10.1016/j.jece.2020.105012>
39. P.G. Carrillo, C. Mardaraz, S.I. Pitta-Alvarez and A.M. Giulietti, *World J. Microbiol. Biotechnol.*, **12**, 82 (1996);  
<https://doi.org/10.1007/BF00327807>
40. S.S. Balan, C.G. Kumar and S. Jayalakshmi, *Process Biochem.*, **51**, 2198 (2016);  
<https://doi.org/10.1016/j.procbio.2016.09.009>
41. I.M.C. Morais, A.L. Cordeiro, G.S. Teixeira, V.S. Domingues, R.M.D. Nardi, A.S. Monteiro, R.J. Alves, E.P. Siqueira and V.L. Santos, *Microb. Cell Fact.*, **16**, 155 (2017);  
<https://doi.org/10.1186/s12934-017-0769-7>
42. S. Deng, G. Yu and Y.P. Ting, *Colloids Surf. B Biointerfaces*, **44**, 179 (2005);  
<https://doi.org/10.1016/j.colsurfb.2005.06.011>
43. K. Okaiyeto, U.U. Nwodo, L.V. Mabinya, A.S. Okoli and A.I. Okoh, *Int. J. Mol. Sci.*, **16**, 12986 (2015);  
<https://doi.org/10.3390/ijms160612986>
44. Y.J. Yin, Z.M. Tian, W. Tang, L. Li, L.Y. Song and S.P. McElmurry, *Bioresour. Technol.*, **171**, 336 (2014);  
<https://doi.org/10.1016/j.biortech.2014.08.094>
45. V. Bisht and B. Lal, *Front. Microbiol.*, **10**, 1288 (2019);  
<https://doi.org/10.3389/fmicb.2019.01288>
46. P. Parthipan, E. Preetham, L.L. Machuca, P.K. Rahman, K. Murugan and A. Rajasekar, *Front. Microbiol.*, **8**, 237675 (2017);  
<https://doi.org/10.3389/fmicb.2017.00193>
47. V.V. Chandanshive, S.K. Kadam, R.V. Khandare, M.B. Kurade, B.H. Jeon, J.P. Jadhav and S.P. Govindwar, *Chemosphere*, **210**, 968 (2018);  
<https://doi.org/10.1016/j.chemosphere.2018.07.064>
48. I. Haq, A. Raj and Markandeya, *Chemosphere*, **196**, 58 (2018);  
<https://doi.org/10.1016/j.chemosphere.2017.12.153>
49. N. Garg, A. Garg and S. Mukherji, *J. Environ. Manage.*, **263**, 110383 (2020);  
<https://doi.org/10.1016/j.jenvman.2020.110383>
50. P. Kaur, J.P. Kushwaha and V.K. Sangal, *J. Hazard. Mater.*, **346**, 242 (2018);  
<https://doi.org/10.1016/j.jhazmat.2017.12.044>
51. M.B. Ceretta, Y. Vieira, E.A. Wolski, E.L. Foletto and S. Silvestri, *J. Water Process Eng.*, **35**, 101230 (2020);  
<https://doi.org/10.1016/j.jwpe.2020.101230>
52. P.S. Patil, U.U. Shedbalkar, D.C. Kalyani and J.P. Jadhav, *J. Ind. Microbiol. Biotechnol.*, **35**, 1181 (2008);  
<https://doi.org/10.1007/s10295-008-0398-6>